Available online at www.sciencedirect.com
SCIENCE DIRECT®
Journal of Molecular Catalysis A: Chemical 207 (2004) 123–129
JOURNAL OF MOLECULAR CATALYSIS A: CHEMICAL
www.elsevier.com/locate/molcata

# Bromoanthracenes and metal co-catalysts for the autoxidation of *para*-xylene

Basudeb Saha, James H. Espenson*

*Ames Laboratory and Department of Chemistry, Iowa State University of Science and Technology, Ames, IA 50011, USA*

Received 6 May 2003; received in revised form 26 June 2003; accepted 27 June 2003

**Abstract**

The autoxidation of *para*-xylene (*p*X) was carried out with the usual $Co(OAc)_2$ catalyst in HOAc, but with promoters other than inorganic bromide. 9,10-Dibromoanthracene and 9-bromoanthracene were used. They gave acceptable rates and yields of terephthalic acid, particularly with low concentrations of metal co-catalysts. The ones studied and their optimal concentrations are 0.3 mM $Mn(OAc)_2$, 0.2 mM $Ce(OAc)_3$ and 20 mM $ZrOCl_2$. The mechanism involves formation of an intermediate radical such as $DBA^{\bullet+}$, which oxidizes *p*X to $pX^{\bullet+}$, a strong acid that rapidly releases $H^+$. Under oxygen, peroxyl radicals are formed, which sustain the free radical branching chains. The redox-active metals Mn(II) and Ce(III) accelerate the reaction because they are oxidized by $ArCH_2OO^\bullet$ ca. $10^3$-times more rapidly than Co(II) is. A different mechanism operates for Zr(IV). By prior addition of *t*-BuOOH, evidence has been obtained for the intervention of peroxo-zirconium(IV) complexes of this $d^0$ metal.


*Keywords:* Autoxidation; *para*-Xylene; Terephthalic acid; Dibromoanthracene; 9-Bromoanthracene

## 1. Introduction

The aerobic oxidation of *para*-xylene is carried out commercially on the scale of $>10^9$ kg annually. The most widely used commercial catalyst package combines $Co(OAc)_2$, $Mn(OAc)_2$ and NaBr or HBr [1–5].

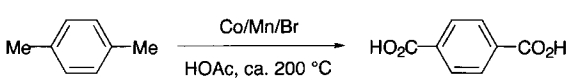

(1)

The autoxidation mechanism has been extensively studied [3,6–15], and shown to be a multi-step process with chain-branching reactions of aralkylperoxyl radicals, $ArCH_2OO^\bullet$. When bromide is used as a promoter, the dibromide radical $HBr_2^\bullet$ is an active intermediate [10,16], Bromide is not without its problems, however, principally its corrosive nature that requires expensive titanium-clad reactors [17]. Minimizing solvent oxidation to CO and $CO_2$ and completion of the oxidation of 4-carboxybenzaldehyde (4-CBA) are further objectives, whether or not bromide is responsible for them.

For these reasons we have studied other promoters to be used in place of inorganic bromide. In this study, we describe results obtained with 9,10-dibromoanthracene (DBA) and 9-bromoanthracene (9-BA). The reaction rates in these systems can be considerably enhanced by the use of co-catalysts such as Mn(II), Co(III) and Zr(IV) by mechanisms that have been characterized to a great extent. We are aware of bromobenzene having been used in this capacity [18], but believe this is the first instance in which bromoanthracenes have been employed.

## 2. Experimental section

The following reagents were used as obtained commercially without further purification: cobalt(II) acetate tetrahydrate, glacial acetic acid, sodium bromide, DBA, 9-BA, zirconyl chloride octahydrate, manganese(II) acetate, cerium(III) acetate, *p*-xylene and *p*-toluic acid. Cobalt(III) acetate solution in glacial acetic acid was prepared by passing ozone gas through a freshly prepared solution of $Co(OAc)_2{\cdot}4H_2O$ [16,19]. The excess ozone was sparged from the solution with a vigorous stream of argon gas. The predominant species was the Co(III)s form

* Corresponding author. Tel.: +5152945730; fax: +5152945233.
*E-mail address:* epenson@iastate.edu (J.H. Espenson).

1381-1169/$ – see front matter © 2003 Elsevier B.V. All rights reserved.
doi:10.1016/S1381-1169(03)00490-4

(a hydroxo-bridged Co(III) dimer) [20], as confirmed by its characteristic UV-Vis spectrum [21].

Reactions were monitored by measuring oxygen consumption with a manometric apparatus similar to the one described in the literature [22]. The reactor was thermostated by means of a circulating water bath at 70 °C. Oxygen consumption was measured by monitoring the decrease in volume (at 1 bar) of pure oxygen in a burette connected to the reactor. From the data so collected the initial reaction rates were calculated with the program KaleidaGraph 3.5.

Oxidation products were detected by HPLC, having calibrated the method, qualitatively and quantitatively, with known compounds. For HPLC analysis, a 0.02 ml aliquot was removed from the reactor at different times during the reaction and diluted to 1 ml in 1:4 DMSO/$CH_3CN$ (v/v) mixture. The diluted solution was then run through the HPLC column. A Waters model 501 solvent delivery system, Waters 996 photodiode array detector and a Novapak $C_{18}$ 3.9 mM × 150 mM column were used for this purpose. A binary solvent of 50% $H_2O$/0.5% $CH_3COOH$ and 50% $CH_3CN$ with a flow rate of 0.7 ml $min^{-1}$ was used in the isocratic mode. Each peak of the HPLC chromatogram was properly integrated and the actual concentration of each component was obtained from the pre-calibrated plot of its peak area versus concentration.

The kinetics of reduction of Co(III) by DBA and 9-BA was followed using Shimadzu UV-2101PC or UV-3101PC spectrophotometers. The progress of the reaction was determined by monitoring the decrease of the Co(III) absorbance at 523 nm. A quartz cell of 1.0 cm path length was used for absorbance measurement.

## 3. Results

### 3.1. Oxidation of para-xylene (pX) with DBA and 9-BA as promoters

In oxygen uptake experiments, the initial change in the volume of $O_2$ was a linear function of time after an initial induction period during which essentially no oxygen was consumed. Fig. 1 presents the data for a typical experiment with these concentrations: 820 mM *p*X, 40 mM Co(II) and 10 mM DBA. The reaction was followed until ca. 15 ml of $O_2$ had been consumed, which amounts to ca. 5% oxidation of *p*X.

The slope of the line gives the initial reaction rate; when converted to concentration units, $v_i = 10.5 \times 10^{-6}$ mol $l^{-1}$ $s^{-1}$. Analogous experiments with 9-BA showed $v_i = 8.1 \times 10^{-6}$ mol $l^{-1}$ $s^{-1}$. These rates are not much larger than the value $v_i = 7.1 \times 10^{-6}$ mol $l^{-1}$ $s^{-1}$ when 10 mM NaBr was used. A series of such experiments was carried out with varying concentrations: 20–80 mM Co(II), 0.4–1.5 M *p*X and 1.7–20 mM DBA. From series in which two of the three concentrations were held constant, the reaction is second-order with respect to [Co(II)] and first-order with respect to [*p*X]. The dependence on

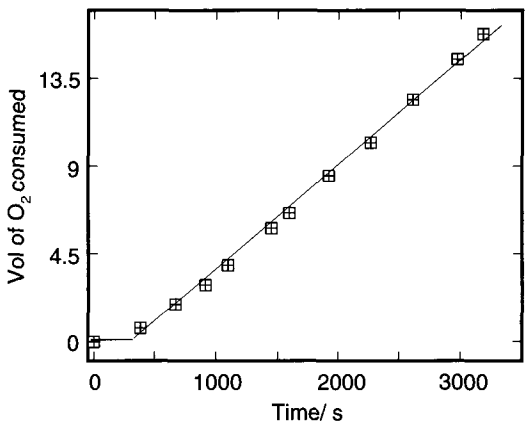


Fig. 1. Plot of the volume of $O_2$ (in ml) consumed as a function of time in an experiment with these concentrations: 820 mM *p*X, 40 mM Co(II) and 10 mM DBA at 70 °C in HOAc.

[DBA] followed saturation kinetics. These three functional dependences can be combined into one rate law,

$$v = k\frac{[\mathrm{Co(II)}]^2[\mathrm{pX}][\mathrm{DBA}]}{1 + \kappa[\mathrm{DBA}]} \quad (2)$$

The initial rate data from oxygen-uptake experiments are precise to only ca. ±20%. The data from 15 experiments were fitted to this equation. The least-squares parameters are $k = 2.8 \pm 1.3\ l^2\ mol^{-2}\ s^{-1}$ and $\kappa = (3.0 \pm 2.0) \times 10^2\ l\ mol^{-1}$. A comparison between experimental and fitted initial rates is given in Fig. 2. As one can see, the kinetic model has its limitations.

Studies with a number of methyl benzenes were carried out with the Co(II)–DBA combination, under comparable conditions, 820 mM $Me_nC_6H_{6-n}$, 40 mM Co(II) and 10 mM DBA. The initial rates increased with the number of methyl groups, which is the order in which $E^\circ$ decreases for the $Me_nC_6H_{6-n}{}^{\bullet+}/Me_nC_6H_{6-n}$ couples. The plot of $\log(v_i)$ against $E^\circ$ is linear, as shown in Fig. 3.

Further experiments were carried out to explore the mechanism of oxidation of *p*X by the combination $Co(OAc)_2$

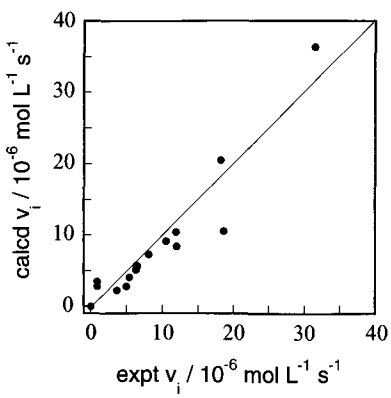


Fig. 2. A comparison of initial rates for the oxidation of *p*X with a Co(II) catalyst and DBA as promoter, showing experimental and fitted data. The straight line has a 45° slope.

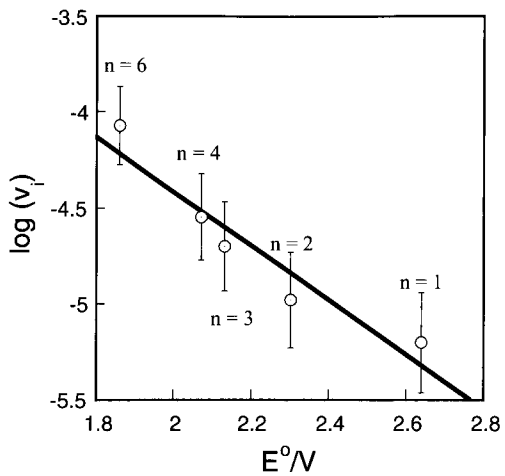


Fig. 3. Plot of the initial rate (log scale) of autoxidation of 0.82 M methylbenzenes, $Me_nC_6H_{6-n}$, catalyzed by 40 mM $Co(OAc)_2$ in the presence of 10 mM 9,10-dibromoanthracene, vs. $E^\circ$ for the couples $Me_nC_6H_{6-n}{}^{\bullet+}/Me_nC_6H_{6-n}$.

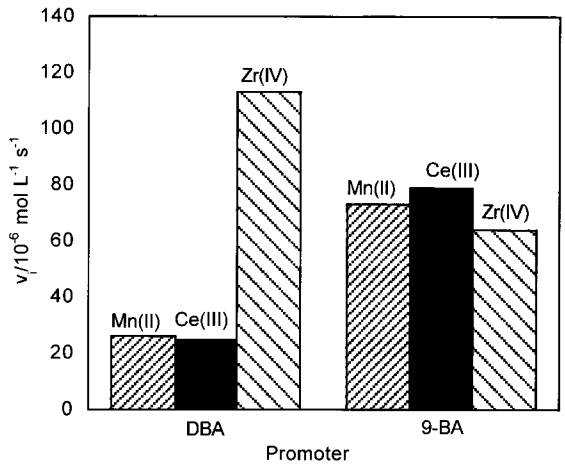


Fig. 4. Initial rates at optimal co-catalyst concentrations—0.3 mM Mn(II), 0.2 mM Ce(III) and 20 mM Zr(IV)—for the DBA (10 mM) and 9-BA (10 mM) promoted autoxidations of *p*X at 70 °C in HOAc.

and DBA. An experiment was performed with 820 mM *para*-xylene-$d_{10}$, 40 mM Co(II) and 10 mM DBA. No kinetic isotope effect (KIE) was observed: $v_{i(H)}/v_{i(D)} = 1.0$. A large KIE had been reported, however, for the oxidation of *p*X by the dibromide radical, $HBr_2^\bullet$, which indicates that $HBr_2^\bullet$ reacts by a hydrogen atom abstraction mechanism [10], and DBA does not.

### 3.2. Formation and oxidation of para-toluic acid

The immediate product of the oxidation of *p*X with these promoters is *para*-toluic acid. Once one methyl group has been oxidized, the remaining one is deactivated by the electron withdrawing effect of the $-CO_2H$ group [11,23]. To explore this further, *p*-$MeC_6H_4CO_2H$ was used directly. With 820 mM substrate, 40 mM Co(II) and 10 mM DBA, $v_i$ ($\times 10^{-6}$ mol $l^{-1}$ $s^{-1}$) = 7.9 at 70 °C. The same experiment with 10 mM NaBr in place of DBA had $v_i$ ($\times 10^{-6}$ mol $l^{-1}$ $s^{-1}$) = 1.9. Thus, DBA is a superior promoter for the step which *para*-toluic acid is oxidized.

### 3.3. Kinetic effects of other metals

Mn(II), Ce(III) and Zr(IV) are known to accelerate the reaction with a bromide promoter in a manner that shows strongly synergistic rate enhancements. To find the best conditions, the Mn(II), Ce(III) and Zr(IV) concentrations were varied in the ranges of 0.1–5, 0.1–5 and 5–20 mM, respectively, at fixed concentrations of promoters (10 mM), Co(II) (40 mM) and *p*X (820 mM). The effects of these metals with the bromoanthracene promoters are quite pronounced, as shown in Fig. 4. In each case the rate attains a maximum value at a particular concentration of the co-catalyst and then declines.

The role of Zr(IV) was explored further, because it seemed to us that its role might be to form peroxo complexes with $ArCH_2OOH$ generated in situ during the experiment. We thus carried out experiments in with *tert*-butyl hydroperoxide (a stand-in for the $ArCH_2OOH$ intermediate) was added to the Co/DBA catalyst system. When $ZrOCl_2$ and *t*-BuOOH were pre-mixed, the reaction started immediately without an induction period. On the other hand, when only $ZrOCl_2$ was added, a considerable induction period was noted. In both cases, however, the initial rate reached the same value, $77 \pm 2 \times 10^{-6}$ mol $l^{-1}$ $s^{-1}$ at 70 °C in HOAc, as shown in Fig. 5. This is an eight-fold increase caused by 15 mM Zr(IV).

### 3.4. Product identification by HPLC

Experiments were carried out on reactions starting with *p*X, 10 mM of the desired promoter and the

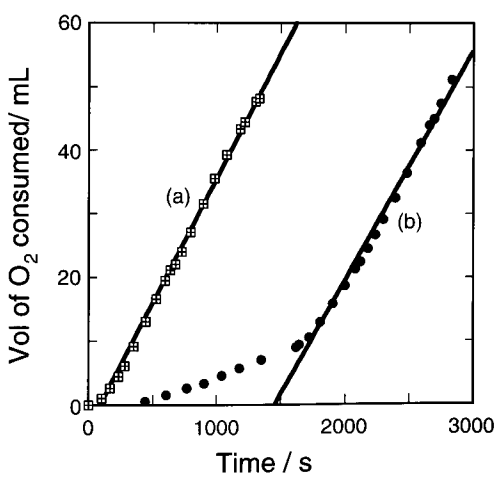


Fig. 5. Plots of oxygen consumption against time when (a) 5 mM *t*-BuOOH was premixed with $ZrOCl_2$ and (b) $ZrOCl_2$ alone was added. Conditions: 40 mM Co(II), 10 mM DBA, 15 mM $ZrOCl_2$, 820 mM *p*-xylene at 70 °C in HOAc.

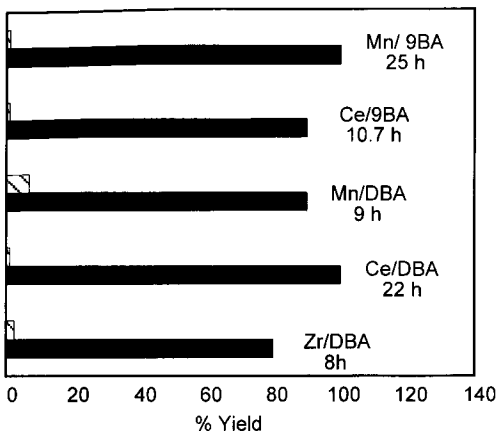


Fig. 6. Yields of *para*-toluic acid (hatched) and terephthalic acid (solid) formed from the autoxidation with use of $Co(OAc)_2$ catalyst, DBA and 9-BA promoters and traces of metal co-catalysts present at their optimal concentrations (Fig. 4).

optimum concentration (0.15–0.3 mM) of Mn(II) or Ce(III) co-catalyst at 70 °C. 4-Methyl-benzyl alcohol was detected directly, despite its lower molar absorptivity at 254 nm as compared to the other intermediates. *p*-Tolualdehyde was formed in an early stage, followed by 70–100% of *p*-toluic acid in 1.3–3 h. The subsequent oxidation led to 4-CBA and terephthalic acid, especially the latter. The yields of the final products are displayed in Fig. 6.

### 3.5. Release of bromide ions

Over time, both DBA and 9-BA do lose bromide during the course of the reaction as anthroquinone (AQ) is formed.

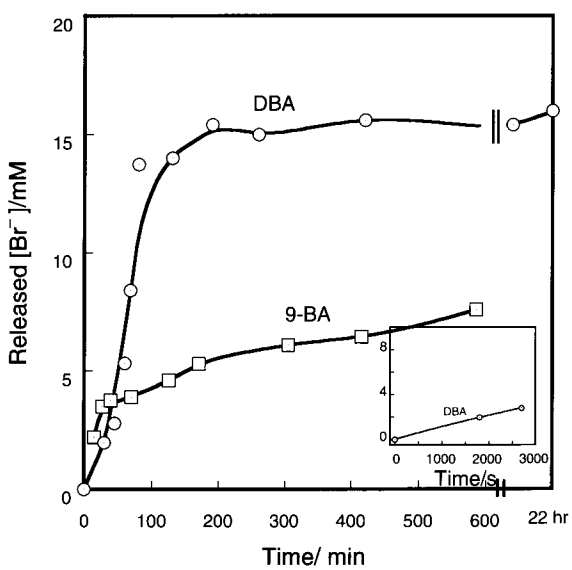


Fig. 7. Plots of released bromide as a function of time for DBA and 9-BA with 40 mM $Co(OAc)_2$, 10 mM DBA or 9-BA, 0.3 mM $Mn(OAc)_2$, and 100 mM *p*X. Inset: bromide formation during the time used for the kinetic measurements.

This decomposition process was followed by HPLC from the measurement of [AQ], retention time 8.7 min, as a function of time. These measurements were performed with added $Mn(OAc)_2$, giving the results shown in Fig. 7. Independently, it was shown that added AQ (10 mM) had no effect on the rate.

Given these results, one must ask whether DBA and 9-BA simply provide a means of introducing HBr into the system, which then acts as the promoter. This cannot be so to any substantial extent because the amount of bromide released during the kinetic period is quite small; see Fig. 7, inset.

During the experiments to measure the KIE, bromide has also not risen to a level where its pathway contributes much to the rate. Indeed, the directly-studies rate of reaction between the $HBr_2^\bullet$ intermediate and *p*X has KIE = 5.3 [10], whereas $k_H/k_D = 1.0$ for *p*X and *p*X-$d_{10}$ with DBA as the promoter.

## 4. Discussion

### 4.1. The chemical mechanism

To place our new results in context, it is useful to recapitulate briefly what is known about the autoxidation of methylarenes ($ArCH_3$) with a $Co(OAc)_2$ catalyst and NaBr promoter. The reaction follows a free-radical scheme in which chain-branching provides one key aspect.

The initiation step generates the chain-carrying radicals. The initiator is the small concentration of the aralkyl hydroperoxide that is present in the hydrocarbon which is reduced by Co(II) in this reaction:

$$ArCH_2OOH + Co(II)Br_2 \rightarrow ArCH_2O^\bullet + HOCo(III)Br_2 \quad (3)$$

We have independently demonstrated that it is the dibromocobalt(II) complex which reacts at this step. The reason for that is to provide a pathway for formation of the reactive dibromide radical, $HBr_2^\bullet$. Here and elsewhere in writing these equations, coordinated acetate ions and acetic acid are being omitted. Also, the Co species are written as monomers, even though dimers and trimers are prevalent in HOAc. especially in aged solutions. Once the reaction begins, however, monomeric Co(IIIa) is formed and it presumably cycles so rapidly as to carry repeated cycles of reaction.

The radical $ArCH_2O^\bullet$ from reaction (3) is highly reactive, and it converts $ArCH_3$ to an aralkyl radical. In so doing the first stage of oxidation has been completed with the formation of an alcohol.

$$ArCH_2O^\bullet + ArCH_3 \rightarrow ArCH_2OH + ArCH_2^\bullet \quad (4)$$

$$ArCH_2^\bullet + O_2 \rightarrow ArCH_2OO^\bullet \quad (5)$$

It is at this stage that chain-branching occurs. A single peroxyl radical becomes three by the sequence of pathways

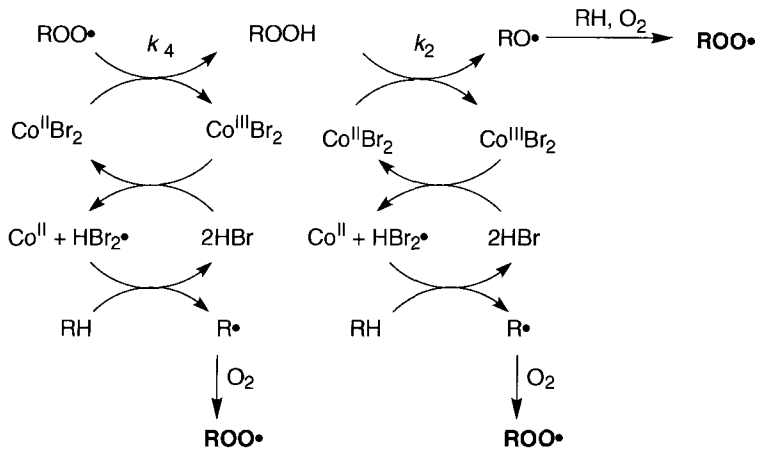


Scheme 1. Chain-branching of peroxyl radicals, R: $ArCH_2$; see [12–14] and [31].

shown in Scheme 1. Without branching, the process would be unacceptably slow.

The dibromide radical formed from inorganic bromide is shown in Scheme 1 as reacting with $ArCH_3$. This step was studied directly by laser flash photolysis, and thus confirmed independently [10]. In HOAc at 23 °C, the rate constant for $HBr_2^\bullet + pX$ is $1.6 \times 10^5$ l mol$^{-1}$ s$^{-1}$, and a significant KIE, $k_H/k_D = 5.3$.

The chain termination step is the self-reaction of the peroxyl radical by the Russell mechanism [24],

$$2ArCH_2OO^\bullet \rightarrow ArCHO + ArCH_2OH + O_2 \quad (k_6) \qquad (6)$$

where the numbering of rate constants here and in Scheme 1 corresponds to prior usage [25]. When the rates of chain-branching and termination become equal, the maximum (steady-state) rate is realized:

$$2\{k_4[Co(II)] + k_2[ArCH_3]\} = 2k_6[ArCH_2OO^\bullet] \qquad (7)$$

As a result the steady-state concentration of the peroxyl radical is

$$[ArCH_2OO^\bullet]_{ss} = \frac{k_4[Co(II)] + k_2[ArCH_3]}{k_6} \qquad (8)$$

It follows that

$$v = \frac{2\{k_4[Co(II)] + k_2[ArCH_3]\}^2}{k_6} \qquad (9)$$

where the reaction rate is defined as $-d[O_2]/dt$ during the initial phase of the oxidation.[1] The reaction rate was found to be nearly second-order with respect to [Co(II)]; it is roughly independent of $[ArCH_3]$. Rate constants were obtained from the chemiluminescence produced because the aldehyde formed in the termination step is in an excited state. This leads to these values of $k$ (l mol$^{-1}$ s$^{-1}$): $k_4 = 7.2 \times 10^2$ (for $Co(OAc)_2$, but higher for $CoBr_2$), $k_2 = 4.5$, and $k_6 = 1.5 \times 10^8$ at 70 °C in HOAc [12]. Therefore, the $k_2$ component of reaction (9) contributes relatively little, and the reaction rate is dominated by the nearly-quadratic Co(II) dependence.

### 4.2. Evidence for electron transfer

The absence of a KIE for the DBA-promoted reaction and the significant dependence of the rate upon the $E^\circ$ values for $Me_nC_6H_{6-n}$ have been noted. They suggest the involvement of coupled electron transfer steps. To assist this discussion it is useful to have values of the standard reduction potentials and the series of steps we propose to be involved, which is shown in Scheme 2. These values of $E^\circ$ in HOAc pertain in this case: Co(III)/Co(II), 2.0 V [26]; DBA$^{\bullet+}$/DBA, 1.76 V [27] and $pX^{\bullet+}/pX$ 2.30 V [28].

The analysis of the steps in Scheme 2 proceeds as follows. Cobalt(III) can oxidize DBA ($K_1 = 10^4$). The rate constant $k_1$ was evaluated directly as $0.67 \pm 0.04$ l mol$^{-1}$ s$^{-1}$ at 25 °C in HOAc. Although the subsequent oxidation of $pX$ by DBA$^{\bullet+}$ is unfavorable ($K_2 = 7 \times 10^{-10}$), it is drawn to completion by the high acidity of $p$-$MeC_6H_4CH_3^{\bullet+}$ ($pK_a = -8$) [29] and its large rate constant for proton loss, $k_3 = 1 \times 10^7$ s$^{-1}$ [30]. The role of DBA is to provide a facile initial electron transfer step, which $pX$ cannot do, given the $E^\circ$ values. The formation of $pX^{\bullet+}$ in a step that equilibrates at a diffusion-controlled rate ($k_2 \sim 10$, $k_{-2} \sim 10^{10}$ l mol$^{-1}$ s$^{-1}$) allows $ArCH_2^\bullet$ to form, from which the key peroxyl radical then results.

A parallel scheme can be written for 9-BA with different values of $K_1$ ($4 \times 10^5$) and $K_2$ ($2 \times 10^{-11}$), but with the product $K_1 \cdot K_2$ ($\sim 7 \times 10^6$) necessarily the same.

Even though DBA and 9-BA release bromide ions during the conversion of $pX$ to terephthalic acid, this may not be entirely disadvantageous. In that way a smaller amount of bromide becomes tied up in the inactive form $ArCH_2Br$, as

[1] Representing the rate in terms of oxygen consumption presents an unavoidable ambiguity, because at different stages of oxidation the stoichiometric consumption ratio of $O_2$ to $pX$ is variable. Complete oxidation to terephthalic acid requires $3O_2$ to $1pX$.

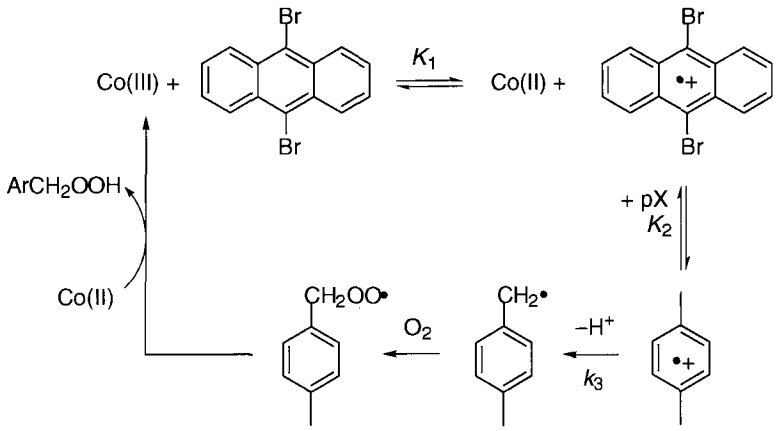


Scheme 2. Postulated role of electron transfer in DBA-promoted reactions.

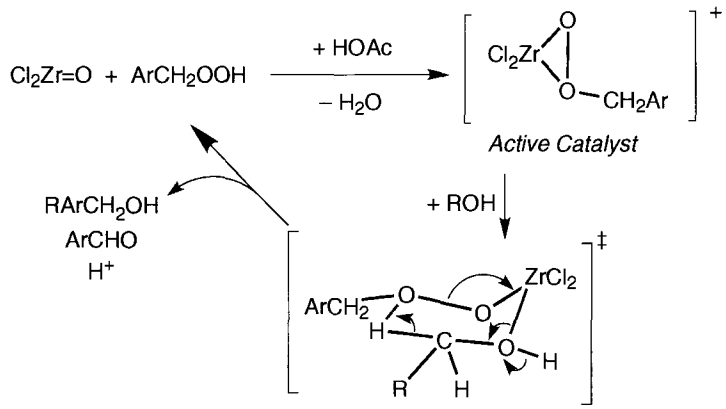


Scheme 3. Proposed involvement of a peroxozirconium intermediate.

compared to the ordinary case where HBr or NaBr is used, where a large fraction of the total bromide is converted to benzylic bromides [31]. The gradual release of bromide ions may promote a greater extent of bromide participation in the chain-branching scheme shown in Scheme 1.

### 4.3. Metal co-catalysts

The roles of the redox-active metals, Mn(II) and Ce(III), can be explained by their participation in chain branching, Scheme 1 [9,14,25]. The rate constant $k_2$ for the step $ArCH_2OO^•$ + M(II) is $10^3$-times faster for Mn(II) than Co(II) [12]. This can be explained by the lower reduction potentials: 1.54 V for Mn(III/II) and 1.61 V for Ce(IV/III). The Mn reactions appear to bifurcate as well, which is why the rate passes through a maximum at an optimal [Mn(II)]. These are the steps involved:

The addition of $ZrOCl_2$ to the reaction increases the rate proportional to [Zr]. Because zirconium is not redox-active, an explanation different from that given for Mn and Ce must be presented for its considerable rate effect must be sought. The idea originally advanced was that it was able to insert into, and thus disrupt, the oligomeric structures of cobalt acetates, increasing the proportion of the more active monomeric forms of cobalt [32]. We wish to suggest an alternative, based on the propensity of metal complexes with $d^0$ electronic configurations to bind and activate hydrogen peroxide and alkyl hydroperoxides [33,34]. This model is supported by the data in Fig. 5, which show that prior addition of *t*-BuOOH eliminates the induction period when $ZrOCl_2$ is used as the co-catalyst. This provides a positive indication that some intermediate species is building up to a significant level during that time. We suggest that it is $ArCH_2OOH$. Peroxo complexes of Zr(IV) [35] and other

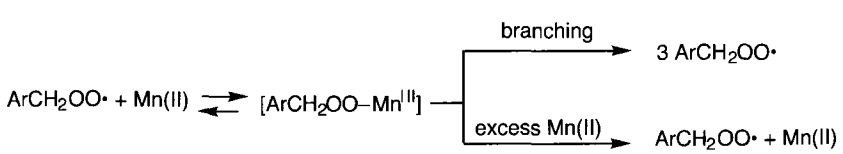


(10)

$d^0$ metal complexes [33,36] have been reported. The fact that experiments with and without pre-added *t*-BuOOH ultimately reached the same rate are indicative of hydroperoxide involvement. Scheme 3 shows a mechanism from the literature that proposes a pathway for the catalyzed oxidation of alcohols by alkyl hydroperoxides [37]. Possibly the intermediate aldehydes (as hemiacetals?) are also oxidized by hydroperoxo-zirconium species.

## Acknowledgements

The authors acknowledge support from BP-Amoco Chemicals. This research was in part carried out in the facilities of the Ames Laboratory of the US Department of Energy, Office of Basic Energy Sciences, Division of Chemical Sciences under contract W-7405-Eng-82 with Iowa State University of Science and Technology.

## References

[1] Y. Yoshino, Y. Hayashi, T. Iwahama, S. Sakaguchi, Y. Ishii, J. Org. Chem. 62 (1997) 6810–6813 (and references therein).
[2] W.F. Brill, Ind. Eng. Chem. 52 (1960) 837–840.
[3] P. Raghavendrchar, S. Ramachandran, Ind. Eng. Chem. Res. 31 (1992) 453–462.
[4] R.C. Jacob, P.S. Verkey, P. Ratnasamy, Appl. Catal. A.: Gen. 182 (1999) 91–96.
[5] A. Cincotti, R. Orru, G. Cao, Catal. Today 52 (1999) 331–347.
[6] S.A. Chavan, S.B. Halligudi, D. Srinivas, P. Ratnasamy, J. Mol. Catal. A: Chem. 161 (2000) 49–64.
[7] W. Partenheimer, J. Mol. Catal. 67 (1991) 35–46.
[8] G.M. Dugmore, G.J. Powels, B. Zeelie, J. Mol. Catal. A 99 (1995) 1–12.
[9] W. Partenheimer, in: D.W. Blackburn (Ed.), A Chemical Model for the Amoco "MC" Oxidation Process to Produce Terephthalic Acid, Marcel Dekker, Inc., New York, 1990.
[10] P.D. Metelski, J.H. Espenson, J. Phys. Chem. 105 (2001) 5881–5884.
[11] W. Partenheimer, Catal. Today 23 (1995) 69.
[12] I.V. Zakharov, Kinet. Catal. 39 (1998) 485–492.
[13] I.V. Zakharov, Y.V. Geletii, V.A. Adamyan, Kinet. Catal. 32 (1991) 31–37.
[14] I.V. Zakharov, Y.V. Kumpan, Kinet. Catal. 23 (1993) 922–927.
[15] G.H. Jones, J. Chem. Res. (1982) 207.
[16] X. Jiao, J.H. Espenson, Inorg. Chem. 39 (2000) 1549–1554.
[17] J.L. Broeker, W. Partenheimer, B.I. Rosen, United Sates Patent No. 05453538 (1994).
[18] I.V. Zakharov, V.M. Muratov, Doklady Akademii Nauk SSSR 196 (1971) 1125–1128.
[19] S.S. Lande, J.K. Kochi, J. Am. Chem. Soc. 90 (1968) 5196–5207.
[20] J.R. Chipperfield, S. Lau, D.E. Webster, J. Mol. Catal. 75 (1992) 123.
[21] W. Partenheimer, R.K. Gipe, in: S.T. Oyama, J.W. Hightower (Eds.), Nature of the Co-Mn-Br Catalyst in the Methyl Aromatic Compounds Process, 1993.
[22] N.M. Emanuel, E.T. Denisov, Z.K. Mazius, Liquid-Phase Oxidation of Hydrocarbons, 1967, p. 350.
[23] B. Cornils, W.A. Herrmann, Applied Homogeneous Catalysis with Organometallic Compounds, VCH, New York.
[24] G.A. Russell, J. Am. Chem. Soc. 79 (1957) 3871–3877.
[25] I.V. Zakharov, Y.V. Geletii, V.A. Adamyan, Kinet. Catal. 29 (1988) 924–929.
[26] V.A. Adamian, private communication, as cited in footnote 1.
[27] J.M. Masnovi, E.A. Seddon, J.K. Kochi, Can. J. Chem. 62 (1984) 2552–2559.
[28] J.O. Howell, J.M. Goncalves, C. Amatore, L. Klasinc, R.M. Wightman, J.K. Kochi, J. Am. Chem. Soc. 106 (1984) 3968–3976.
[29] W. Lau, J.K. Kochi, J. Am. Chem. Soc. 106 (1984) 7100–7112.
[30] T.D. Giacco, E. Baciocchi, S. Steenken, J. Phys. Chem. 97 (1993) 5451–5456.
[31] P.D. Metelski, V.A. Adamian, J.H. Espenson, Inorg. Chem. 39 (2000) 2434–2439.
[32] A.W. Chester, E.J.Y. Scott, P.S. Landis, J. Catal. 46 (1977) 308–319.
[33] G. Strukul, Kluwer Academic Publishers, Dordrecht.
[34] J.H. Espenson, Chem. Commun. (1999) 479–488.
[35] R.C. Thompson, Inorg. Chem. 24 (1985) 3542–3547.
[36] H. Adam, K. Khanbabaee, K. Krohn, J. Kupke, H. Rieger, K. Steingrover, I. Vinke, in: W. Adam (Ed.), Transition-Metal Alkoxide-Catalyzed Oxidation of Phenols, Alcohols, and Amines with *tert*-Butyl Hydroperoxide, Wiley-VCH, New York, 2000.
[37] K. Krohn, L. Vinke, W. Adam, J. Org. Chem. 61 (1996) 1467–1472.